SIZE OPTIMIZATION METHOD FOR FLUTTER INSTABILITY PROBLEMS

Pedro Pastilha, ppastilha@gmail.com
DEM – Instituto Superior Técnico – Portugal.

Olavo M. Silva, olavo@lva.ufsc.br
GTVA – Federal University of Santa Catarina – Florianopolis – Brazil.

Miguel Matos Neves, maneves@dem.ist.utl.pt
Afzal Suleman, suleman@dem.ist.utl.pt
IDMEC – Instituto Superior Técnico – Portugal.

Abstract. *The paper presents finite element analysis and structural optimization methodologies for the problem of flutter instability of a cantilever column subject to the thrust from a single propeller rocket at the free end. The objective of the optimization is to achieve a minimal volume structure while maintaining structural stability within a large interval of excitation frequencies. As a first optimization method, optimal designs are obtained by varying the column's cross-sectional area. Several results where obtained for different loading conditions. In order to further improve the optimized designs topological optimization methods are considered. In order to implement this optimization technique, a finite element analysis is developed considering plate elements and, from this analysis, a larger set of design variables becomes available allowing for entirely new optimal designs.*

Keywords*: Dynamic Stability, Flutter, Follower Loads, Structural Optimization, Beck's Column, Topology Optimization.*

1. INTRODUCTION

The present paper deals with the stability analysis of simple structural elements subjected to non-conservative loads and subsequent optimization procedures in order to minimize structural volume while keeping stability conditions. There are several engineering areas in which non-conservative loads are quite common such as automotive, aeronautics or even space structures. For all these applications the importance of optimal designs is reinforced by the constant need of lighter structures with very high stability requirements.

For the present case, consider a single propeller rocket subjected to thrust and aerodynamic drag, both good examples of partial non-conservative forces. The concept of partial non-conservative force can be explained by considering the rocket propeller from the mentioned structure. While the thrust from the rocket engine is a pure non-conservative force (which may change in direction and magnitude with time and structural geometry variations), the weight of the engine itself is a conservative load (does not change direction or magnitude with time or structural displacement). This complex physical problem can be simplified to the case of a simple cantilevered column subjected to a partial non-conservative force as shown in Fig. 1. Despite generating some controversy (as discussed by Sugiyama *et al.*, 1999), the simplified model allows for insightful and more efficient analysis and optimization studies. In addition, the presented model shows equivalent stability characteristics as a full model and the results have been verified experimentally (by Sugiyama *et al.*, 2000).

When a structure is subjected to the combined action of both conservative and non-conservative forces, different instability modes need to be considered depending on the loading characteristics. The presented work shows that when a uniform cantilever column is subjected to a pure conservative load or when the non-conservative load contribution is relatively small (less than half of the total applied load), the instability mode presents itself as divergence. As the non-conservative load component increases (above half of the total applied load), instability occurs as flutter. Flutter instability can be defined as an unfavorable coupling between dynamic and static loads, which results in the loss of structural stability and, ultimately, structural collapse. The work developed follows the work by Langthjem and Sugiyama (1999, 2000a, 2000b).

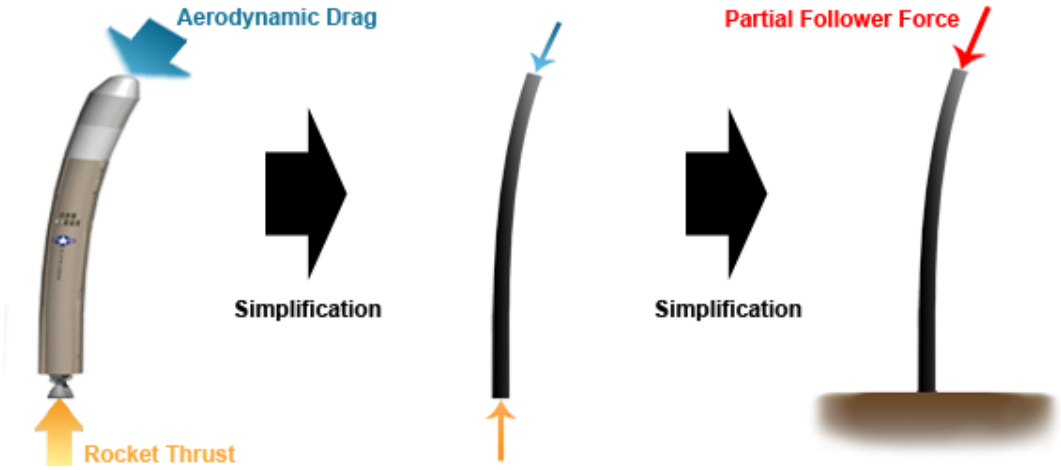

Figure 1. Assumed simplifications for the considered model.

The differential equations describing the behaviour of the presented model are solved using the finite element method and the stability conditions for the column are displayed as load-frequency curves. A first optimization process was implemented, consisting on the minimization of the structural volume by varying the cross-sectional areas of the column while maintaining the stability conditions above the values obtained for the uniform column. For this optimization process the column was modeled using bidimensional beam elements.

With a second optimization procedure in mind, where the structure is optimized using topological optimization procedures, the cantilevered column is modeled using three-dimensional plate elements and the structure and stability results are presented for the uniform case. General studies of plates subjected to distributed follower loads are presented by Kim *et al.* (1998, 2000) and Jayaraman *et al.* (2005). Zuo and Schreyer (1996) developed analysis techniques for divergence and flutter instability of beams and plates subjected to follower forces.

In order to maintain stability conditions, constraints had to be applied to the critical load values during the optimization process. To avoid large jumps in the critical load between the iterative steps of the optimization process, the frequency curves also required constraints. It is known that the stability conditions of a structure subjected to a non-conservative force may not evolve smoothly with small geometry changes. Therefore, the optimization process in these conditions becomes somewhat difficult and requires strong optimization algorithms based on sensitivity analyses in order to determine the derivatives of the objective and constraint functions with respect to the project variables. The optimization process was performed using the method of moving asymptotes developed by Krister Svanberg (1998).

2. MATHEMATICAL MODELS

2.1 Beam Formulation

The mathematical model that describes small amplitude vibrations on a cantilevered column following the Bernoulli-Euler beam theory takes the form,

$$\frac{\partial^2}{\partial x^2}\left(EI\frac{\partial^2 w}{\partial x^2}\right)+p\frac{\partial^2 w}{\partial x^2}+m\frac{\partial^2 w}{\partial t^2}=0 \tag{1}$$

where E is the elasticity modulus, $I = I(x)$ is the area moment of inertia, $w = w(x,t)$ is the transverse displacement at the instant t and at the position x, p is the total load applied to the column and $m = m(x)$ is the mass per unit length. Considering that the load p has two components (conservative and non-conservative, the parameter η is introduced to define the fraction of the total applied load that is non-conservative, as represented in Fig. 2). For a clamped column at $x=0$ and free at $x=L$, the boundary conditions are given by

$$\begin{aligned} &w(x=0,t)=0, \qquad &&\frac{\partial w(x=0,t)}{\partial x}=0 \\ &EI\frac{\partial^2 w(x=L,t)}{\partial x^2}=0, \qquad &&\frac{\partial}{\partial x}\left(EI\frac{\partial^2 w(x=L,t)}{\partial x^2}\right)+p(1-\eta)\frac{\partial w(x=L,t)}{\partial x}=0 \end{aligned} \tag{2}$$

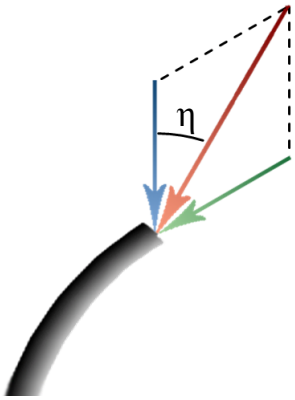

Figure 2. Graphical Representation of the parameter η.

Equations (1) and (2) constitute the complete mathematical model that describes the behavior of the column. For computational simplicity, the previous equations are formulated in a dimensionless form by considering the following dimensionless variables (as considered by Langthjem and Sugiyama, 2000b),

$$\bar{x} = \frac{x}{L},\ \bar{w} = \frac{w}{L},\ \bar{p} = \frac{pL^2}{EI_0},\ \bar{m}(x) = \frac{m_{(x)}}{m_0},\ \bar{I}(x) = \frac{I(x)}{I_0},\ \bar{t} = \frac{t}{L^2}\sqrt{\frac{EI}{m_0}},\ \bar{\omega} = \frac{t}{\bar{t}}\omega \tag{3}$$

From these, the boundary problem described by the equations (1) and (2), takes the following form,

$$\frac{\partial^2}{\partial \bar{x}^2}\left(\bar{I}\frac{\partial^2 \bar{w}}{\partial \bar{x}^2}\right) + \bar{p}\frac{\partial^2 \bar{w}}{\partial \bar{x}^2} - \bar{\omega}^2 \bar{m}\bar{w} = 0 \tag{4}$$

$$\begin{aligned} &\bar{w}(\bar{x}=0) = 0, \qquad \frac{\partial \bar{w}(\bar{x}=0)}{\partial \bar{x}} = 0 \\ &\bar{I}\frac{\partial^2 \bar{w}(\bar{x}=1)}{\partial \bar{x}^2} = 0,\ \frac{\partial}{\partial \bar{x}}\left(\bar{I}\frac{\partial^2 \bar{w}(\bar{x}=1)}{\partial \bar{x}^2}\right) + \bar{p}(1-\eta)\frac{\partial \bar{w}(\bar{x}=1)}{\partial \bar{x}} = 0 \end{aligned} \tag{5}$$

Having defined the dimensionless problem for the beam case the over bars will no longer be used, for notation simplicity. Although it is possible to obtain a semi-analytical solution for this problem, it is only valid for columns with constant mass and stiffness distributions. When considering a column with non-uniform sections, a discretization method is required in order to obtain the solution for these equations.

2.2 Plate Formulation

The behaviour of a isotropic plate subjected to non-conservative loads can be described by the first order shear deformation theory (Reissner-Mindlin plate theory) as follows,

$$\begin{aligned} &\frac{\partial M_x}{\partial x} + \frac{\partial M_{xy}}{\partial x} - Q_x + \frac{h^2}{12}\left(p\frac{\partial^2 \phi_x}{\partial x^2} + h\rho\frac{\partial^2 \phi_x}{\partial x^2}\right) = 0 \\ &\frac{\partial M_{xy}}{\partial x} + \frac{\partial M_y}{\partial y} - Q_y + \frac{h^2}{12}\left(p\frac{\partial^2 \phi_y}{\partial x^2} + h\rho\frac{\partial^2 \phi_y}{\partial x^2}\right) = 0 \\ &\frac{\partial Q_x}{\partial x} + \frac{\partial Q_y}{\partial y} - p\frac{\partial^2 w}{\partial x^2} - h\rho\frac{\partial^2 w}{\partial t^2} = 0 \end{aligned} \tag{6}$$

where Q_x and Q_y are shear forces, M_x, M_y and M_{xy} are bending moments originated by the loading conditions of the structure, ϕ_x and ϕ_y are the rotations of the transverse normal section of the plate. As was the case for the beam

formulation, the plate is clamped at $x=0$ and has an applied partial non-conservative load at the free end ($x=L$). These boundary conditions are introduced into the previous equations in the form,

$$\begin{aligned} &w(x=0,y,t)=0, \qquad \phi_x(x=0,y,t)=0, \qquad \phi_y(x=0,y,t)=0 \\ &Q_x(x=L,y,t)+p(1-\eta)\frac{\partial w(x=L,y,t)}{\partial x}\phi_x(x=L,y,t)=0, \qquad M_x(x=L,y,t)=0 \end{aligned} \tag{7}$$

In order to compare the plate formulation results with the beam model presented, the problem must also be reduced into a dimensionless form. Choosing as a characteristic length the plate dimension in the x direction, the following dimensionless quantities are introduced,

$$\begin{aligned} &\bar{x}=\frac{x}{L},\ \bar{y}=\frac{y}{L},\ \bar{w}=\frac{w}{L},\ \mu=\frac{h}{L}\ \ \bar{p}=\frac{pL^2}{D},\ \bar{t}=\frac{t}{L^2}\sqrt{\frac{D}{\rho h_0}},\ \ \bar{\omega}=\frac{t}{\bar{t}}\omega \\ &\bar{q}_x=\frac{Q_x}{kGh_0},\ \bar{q}_y=\frac{Q_y}{kGh_0},\ \bar{m}_x=\frac{M_x}{kGh_0L},\ \bar{m}_y=\frac{M_y}{kGh_0L},\ \bar{m}_{xy}=\frac{M_{xy}}{kGh_0L} \end{aligned} \tag{8}$$

where $D=Eh_0^{\,3}/12(1-\nu^2)$ is the flexural rigidity of the plate and v is the Poisson ratio. Introducing these dimensionless into equations (6) and (7) results in,

$$\begin{aligned} &\frac{\partial\bar{m}_x}{\partial\bar{x}}+\frac{\partial\bar{m}_{xy}}{\partial\bar{x}}-\bar{q}_x+\frac{r\bar{\mu}^2}{12}\left(\bar{p}\frac{\partial^2\phi_x}{\partial\bar{x}^2}+\bar{\omega}\frac{\partial^2\phi_x}{\partial\bar{t}^2}\right)=0, \qquad \frac{\partial\bar{m}_{xy}}{\partial\bar{x}}+\frac{\partial\bar{m}_y}{\partial\bar{y}}-\bar{q}_y+\frac{r\bar{\mu}^2}{12}\left(\bar{p}\frac{\partial^2\phi_y}{\partial\bar{x}^2}+\bar{\omega}\frac{\partial^2\phi_y}{\partial\bar{t}^2}\right)=0, \\ &\frac{\partial\bar{q}_x}{\partial\bar{x}}+\frac{\partial\bar{q}_y}{\partial\bar{y}}-r\left(\bar{p}\frac{\partial^2 w}{\partial\bar{x}^2}+\bar{\omega}\frac{\partial^2 w}{\partial\bar{t}^2}\right)=0 \end{aligned} \tag{9}$$

$$\begin{aligned} &\bar{w}(\bar{x}=0,\bar{y},\bar{t})=0, \qquad \phi_x(\bar{x}=0,\bar{y},\bar{t})=0, \qquad \phi_y(\bar{x}=0,\bar{y},\bar{t})=0 \\ &\bar{q}_x(\bar{x}=1,\bar{y},\bar{t})-\bar{p}(1-\eta)\frac{\partial\bar{w}(\bar{x}=1,\bar{y},\bar{t})}{\partial\bar{x}}\phi_x(\bar{x}=1,\bar{y},\bar{t})=0, \qquad M_x(\bar{x}=1,\bar{y},\bar{t})=0 \end{aligned} \tag{10}$$

with $r=1/kG\mu L$. The dimensionless form of these equations allows the comparison of the results obtained by both methods, and the stability response of the structure should not change considerably as long as the characteristic dimensions of both models are similar.

The described first order method allows the study of thick plates, which for optimization procedures is an advantage. This model also allows the study of local instability modes as well as torsional stability of the structure, although this is not a main concern for the present work.

3. FINITE ELEMENT ANALYSIS

The discretization of the previously introduced differential equations and corresponding boundary conditions given in dimensionless form by equations (4) and (5) for beam structures and by equations (9) and (10) for plates, are solved using the finite element method. For the beam model, two node isoparametric elements with two degrees of freedom at each node are considered with full integration. For the plate model, four node isoparametric elements are considered with reduced integration and three degrees of freedom at each node. Reduced integration is used to minimize the effects of shear locking verified for thin plates. For the beam case, the column is divided into N_e line elements, each with length l_e and a linear diameter variation given in element coordinates by,

$$m_e=(1-\xi)\mu_e+\xi\mu_{e+1} \tag{11}$$

in which μ_e is the diameter of the beam at node e. For the plate discretization, the structure is divided into Nx elements in the x direction and Ny elements in the y direction, each with a length lx and height ly. The thickness distribution along the element is also assumed to have a linear evolution according to,

$$m_e=(1-\xi)(1-\gamma)\mu_1+(1-\xi)\gamma\mu_2+\xi\gamma\mu_3+\xi(1-\gamma)\mu_4 \tag{12}$$

given in the element local reference frame. Using Hermite cubic interpolation functions for the beam element discretization and Lagrange linear interpolation functions for the plate problem results in the following eigenvalue problem,

$$\mathbf{L}\,\mathbf{u} = \left[\mathbf{K}(\mu) - \omega^2\mathbf{M}(\mu) - p\mathbf{Q}\right]\mathbf{u} = 0 \tag{13}$$

where **K** is the stiffness matrix, **M** is the mass matrix and **Q** is the geometric matrix defining the point at which the load p is applied and considering a non-conservative load component depending on the value of η, μ is a vector with the dimensionless project variables and **u** is a vector containing structural nodal coordinates. Matrices **K** and **M** are real and symmetric, while **Q** is non symmetric for any non-conservative loading condition ($\eta \neq 0$).

The solution for the eigenvalue and eigenvector problem presented by equation (13), for both the beam and plate problems, was implemented in MATLAB in order to obtain the eigenvalue frequency and corresponding modes for any given load p. Evaluating these frequency values, it is possible to identify the loads for which the structure loses rigidity and the corresponding instability mode. For a given load parameter η, when a frequency reaches zero, the instability mode is divergence. Flutter occurs when two frequency values coalesce, resulting also in the loss of structural rigidity.

Figure 3 represents the stability regions for two uniform columns: The first, with circular cross-sections, is modeled with beam elements and the second, modeled with plate elements, has rectangular cross-sections and similar characteristic dimensions. These columns are subjected to various load combinations going from a pure conservative load ($\eta = 0$, an Euler buckling problem) to a pure non-conservative load ($\eta = 1$, Beck's column). From this diagram it is also possible to notice that as divergence turns into flutter, the stability margin also increases significantly. This is mainly because damping effects are not considered in the present analysis, although it can also be verified in a smaller degree for damped structures. Another conclusion that can be taken form the figure is that both the beam and plate models made as adimensionalized "similar" structures produce quite similar results, in spite of the critical loads for the plate model being generally inferior to the ones obtained from the beam model.

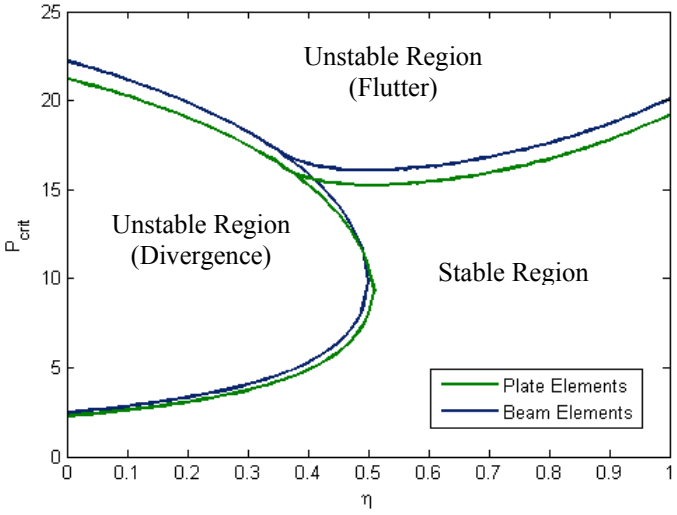

Figure 3. Stability diagram for the uniform columns.

3.1 Stability Results for Beam Elements

As mentioned earlier, flutter occurs when frequency coupling is verified at any given load condition. Thus, one of the most important analysis aspects to consider when studying this type of instability problems is the structural load-frequency response. Figure 4 shows load-frequency curves for the dimensionless uniform column for several load types. The Euler column (conservative load) is shown in figure 4*a)*. The instability mode for this column is divergence and the first critical load occurs at p_{cr}= *2.467*. Figure 4b) represents the structural response for a load with a *25%* non conservative component. For this column, the instability mode is also divergence, and occurs at p_{cr}= *3.651*. When the non-conservative load is 50% of the total load, as represented in figure 4c), the first instability mode is still divergence (at p_{cr} = *9.870*), but flutter instability can now occur at p_{cr} = *16.1*. As shown in figure 4d) flutter is the main instability mode for a 75% follower load, and instability occurs at a load of p_{cr} = *17.2*. Finally, when the load is completely non-conservative we have the problem described by Beck's column, and flutter occurs at p_{cr} = *20.05*. These results show good agreement with the work developed by Langthjem and Sugiyama (2000a). This analysis of the load-frequency response for the structure presents the basis for the optimization analysis described in the next section.

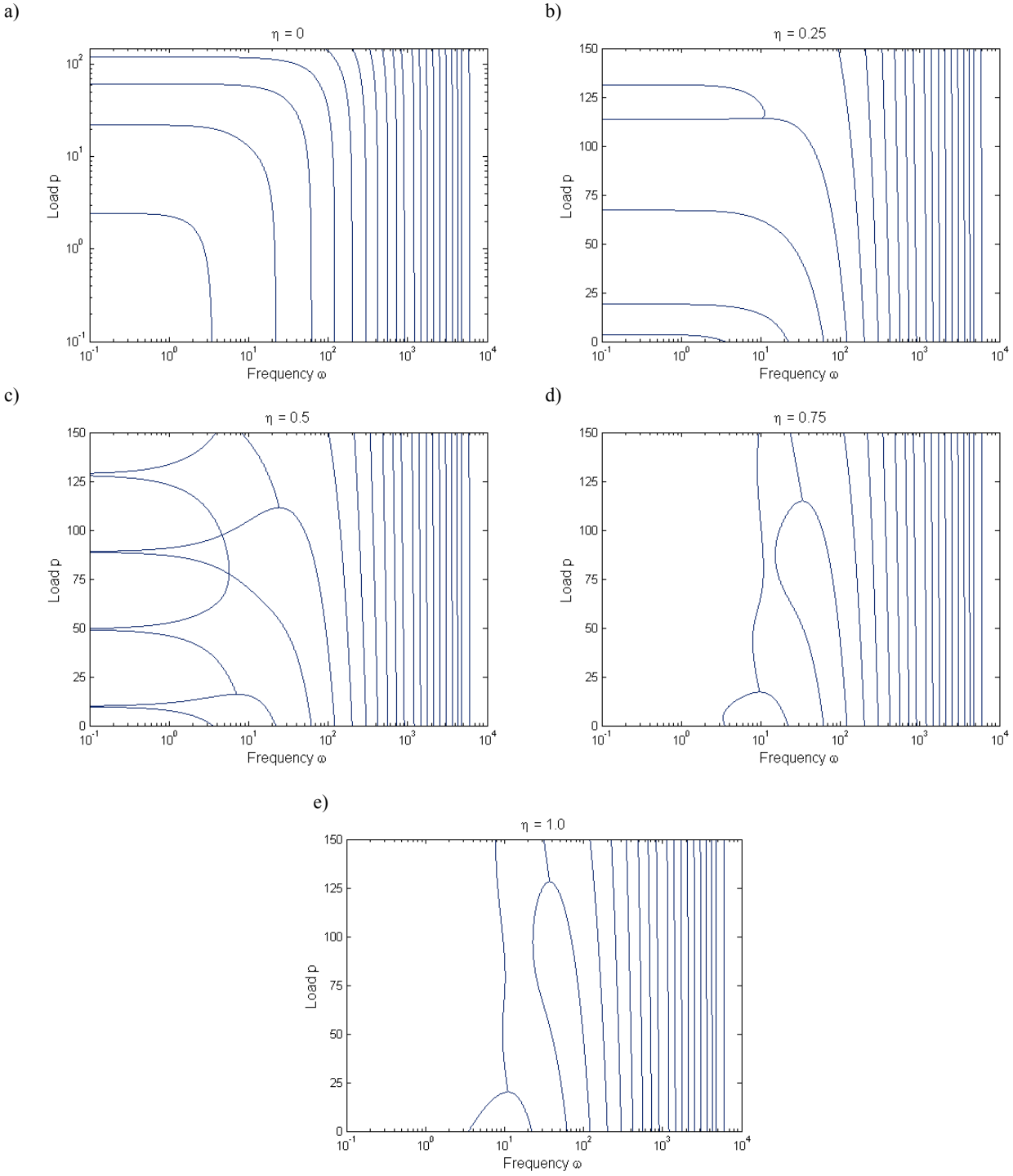

Figure 4. Load Frequency curves for various load types, from a conservative force ($\eta = 0$), to a pure follower load (Beck's column, for $\eta = 1.0$). The results presented were obtained for a uniform column with circular cross sections, modeled with beam elements.

3.2 Stability Results for Plate Elements

Figure 5 shows the load-frequency curves obtained with the plate model described in section 2.2, for a uniform dimensionless column. The considered load values where the same as the ones previously considered for the beam model and the obtained results are considered identical to the ones obtained for the beam model. The main difference between the plots is the presence of torsional frequency modes. As expected, for a plate under a uniform compressive load, the torsional instability loads are very high and, as a consequence, not present in the plots from Figure 5. The instability loads for each load condition are also slightly different from the previously obtained values, in agreement with the results presented in Figure 3. For the Euler column, the first instability mode to occur is divergence at p_{cr} =

2.275 (figure 5a). For a non-conservative contribution of 25% as represented in figure 5b, the instability mode is divergence as well and occurs for a loading of $p_{cr} = 3.363$. Figure 5c shows the case when the non-conservative load component is half of the total applied load. In this case, divergence is the first instability mode to occur, for a load of $p_{cr} = 8.052$. Figure 5d shows the stability curves for a non-conservative contribution of 75% and the main instability mode is now flutter at $p_{cr} = 16.26$. Finally, when the load is completely non-conservative, the dominant instability mode is flutter and the first instability load occurs for $p_{cr} = 19.2$. This stability analysis for the plate model is a starting point for new optimization procedures considering the thickness at each node as project variables.

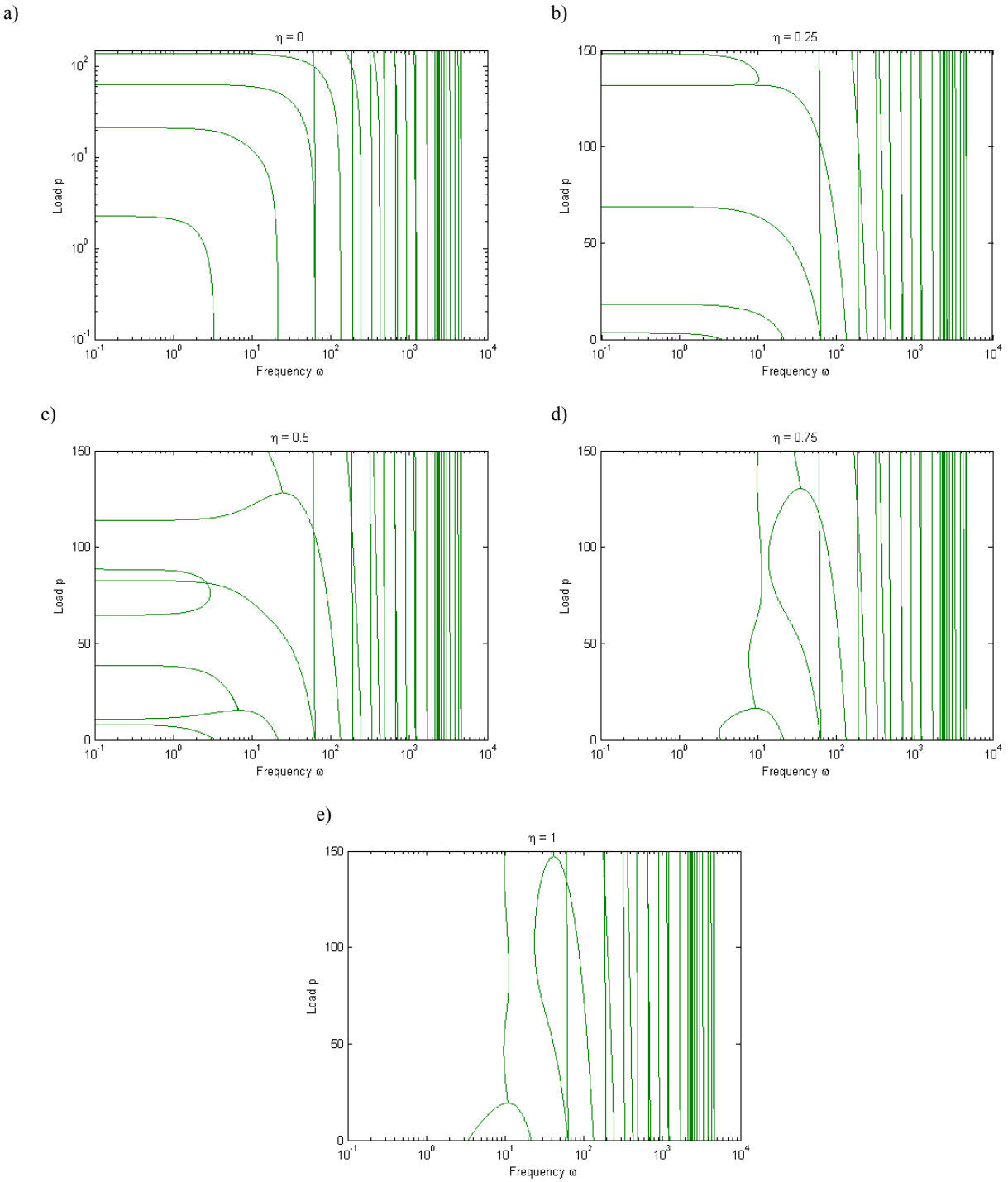

Figure 5. Load Frequency curves for various load types, from a conservative force ($\eta = 0$), to a pure follower load (Beck's column, for $\eta = 1.0$). The results presented were obtained for a uniform column with a rectangular cross-section modeled with plate elements.

4. OPTIMIZATION PROCESS

4.1 Problem Formulation

The optimization problem for the presented structural analysis models can be formulated as follows,

$$\begin{aligned} &\underset{\mu}{\textit{Minimize}} && V, \\ &\textit{subject to} && p_{cr} \geq p_{cr}^{0}, && (14)\\ &&& \omega_{n+1} - \omega_n \geq 0, \quad \forall\ p \leq p_{cr}, && (15)\\ &&& \omega_1 \geq 0, \quad \forall\ p \leq p_{cr}, && (16)\\ &&& \mu_{\min} \leq \mu \leq \mu_{\max}. && (17) \end{aligned}$$

where V is the total structural volume, $\boldsymbol{\mu}$, the project variables vector (diameter for the beam model, thickness for the plate models) and p_{cr}^{0} is the critical load for the uniform column. Constraint (14) is present to avoid large variations on the critical load induced by small changes on the design parameters. Constraint (15) was implemented to prevent flutter instability to change into divergence.

The optimization algorithm for the beam formulation was implemented iteratively using the method of moving asymptotes developed and implemented in MATLAB by K. Svanberg (1998). The iterative process stops when changes in the objective function are under 0.001%. In order to avoid large jumps in the design variables between iterations, limits where imposed. On any iteration, the minimal value for each design variable should not be under 30% of the value of the variable at the previous iteration. Likewise, the maximum value should not be above 30% of the value from the previous iteration. The absolute limits for the design variables, $\mu_{\min}$ and $\mu_{\max}$ were defined as 10^{-5} and 10, respectively.

4.2 Sensitivity Analysis

When implementing a structural optimization process using gradient based methods, it is necessary to perform a sensitivity analysis of the objective and constraint functions with respect to the design variables. The sensitivity analysis method for eigenvalue problems is fully described by Pedersen (1983). The sensitivities for the critical load and frequency values with respect to the design variables are given by:

$$\frac{\partial p_{cr}}{\partial \mu_e} = \frac{\mathbf{u}^T [\mathbf{K}(\mu_e) - \omega^2 \mathbf{M}(\mu_e)]\mathbf{v}}{\mathbf{u}^T [\mathbf{Q}]\mathbf{v}} \tag{18}$$

$$\frac{\partial \omega}{\partial \mu_e} = \frac{\mathbf{u}^T [\mathbf{K}(\mu_e) - \omega^2 \mathbf{M}(\mu_e)]\mathbf{v}}{2\omega\, \mathbf{u}^T [\mathbf{M}]\mathbf{v}} \tag{19}$$

where μ_e are the design variables at element 'e', and $\mathbf{v}$ is the nodal solution vector of the problem adjoint to the finite element formulation presented by equation (13) and it is calculated solving the following algebraic equation,

$$\mathbf{L}^T\ \mathbf{v} = \left[\mathbf{K}(\mu) - \omega^2 \mathbf{M}(\mu) - p\mathbf{Q} \right]^T \mathbf{v} = 0 \tag{20}$$

where the values of p and ω correspond to the point for which the sensitivities are being calculated. The objective function for the optimization problem is the structural volume, calculated for the case of the beam with circular cross-sections, by

$$V = \mathbf{a}^T \mu \ \Rightarrow\ \frac{\partial V}{\partial \mu} = \mathbf{a}, \qquad \mathbf{a} = \left[l_1,\ l_1 + l_2,\ l_2 + l_3,\ \ldots,\ l_{N_{e-1}} + l_{N_e},\ l_{N_e} \right] \tag{21}$$

here, the values of l_e are the element lengths, and $\mathbf{a}$ defines a vector with linear combinations of these elements at each node. On the performed analysis, all element lengths were considered equal and constant during the optimization process. From equation (21) it is possible to verify that the derivative of the objective function with respect to the design variables is constant.

In order to verify the accuracy of the results from the analytical derivatives defined by (18) and (19), they where compared with the numerical approximation given by the finite differences method. Using second-degree finite differences formulas to calculate the approximate solution for the derivatives, it was possible to obtain a very good agreement between analytical and numerical methods, with errors in the order of 10^{-6} %. This study confirms that the analytical expressions for the derivatives are accurate.

4.3 Optimization Results

The optimal structures obtained by the described optimization analysis will now be presented. Results were obtained for the five load conditions considered in section 3 and are summarized in table 1:

Table 1 – Optimization results

Load Condition *(η)*	**Optimal Volume**	**Volume Reduction *(%)***	**Reference [2] results**
0.00	0.866	13.4	0.866
0.25	0.476	52.4	-
0.50	0.473	52.7	0.486
0.75	0.490	50.9	-
1.00	0.374	62.6	0.379

As shown, the optimization process allowed for significant volume reductions while respecting all the imposed constraints. Comparing these results with the work developed by Langthjem and Sugiyama (2000a), it is possible to verify that, for identical load conditions, the optimal results obtained are slightly lower than the ones obtained in the mentioned work. Figure 6 represents the obtained shape of the optimal columns for the results in table 1.

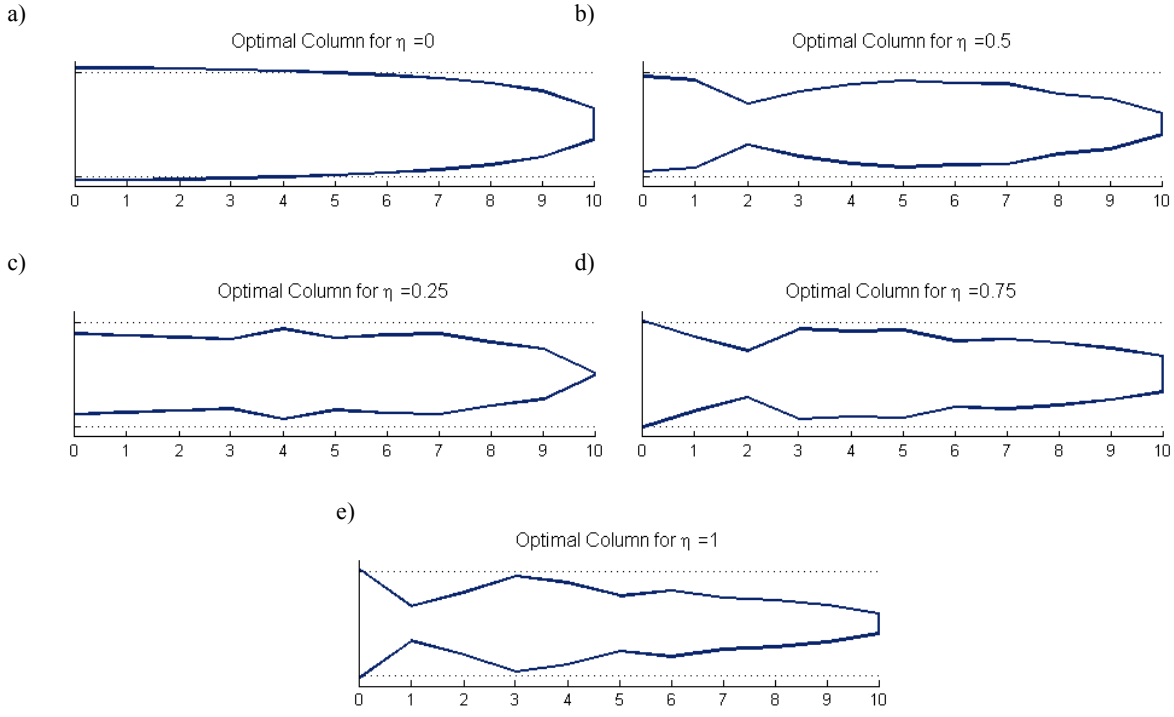

Figure 6. Optimal columns for various non-conservative load parameters. The dashed lines represent the uniform column.

5. CONCLUSIONS AND FURTHER DEVELOPMENTS

From the work described in this article, it is possible to demonstrate the importance of finding optimal design solutions in flutter instability problems, since results show that it is possible to greatly reduce structural weight while maintaining structural stability. When considering applications like aeronautics, where structural weight and volume are an important design issue, large volume reductions as the ones obtained in the present work demonstrate the need for optimal solutions. It was also possible to verify the well-known fact that flutter instability is very sensitive to shape and load variations.

The authors are currently implementing the optimization procedures for the finite element plate model, which are expected to allow for even more efficient optimal designs. As further developments, the inclusion of damping effects and a study on the influence of damping in the optimal designs would be a valuable complement. In addition, the development of optimization techniques considering different loading conditions would also contribute for the verification and validation of these optimization methods.

6. ACKNOWLEDGEMENTS

This work received support from FCT through the project POCTI/EME/ 44728/2002 (MMN), FEDER and IDMEC-IST and CAPS-UFSC (Brazil). The authors are grateful to Prof. Krister Svanberg from Royal Institute of Technology, Stockholm, for providing his MATLAB version of MMA.

7. REFERENCES

Jayaraman, G., Struthers, A., 2005, "Divergence and Flutter Instability of Elastic Specially Orthotropic Plates Subject to Follower Forces", Journal of Sound and Vibration, 281, 357-373.

Kim, J. H., Kim, H. S., 2000, "A Study on the Dynamic Stability of Plates Under a Follower Force", Computers and Structures, 74, 351-363.

Kim, J. H., Park, J. H., 1998, "On the Dynamic Stability of Rectangular Plates Subjected to Intermediate Follower Forces", Journal of Sound and Vibration, 209 (5), 882-888.

Langthjem, M. A., Sugiyama, Y., 1999, "Optimum Design of Beck's Column with a Constraint on the Static Buckling Load", Structural Optimization, 18, 228-235.

Langthjem, M. A., Sugiyama, Y., 2000a, "Optimum Design of Cantilevered Columns Under the Combined Action of Conservative and Nonconservative Loads, Part I: The Undamped Case", Computers and Structures, 74, 385-398.

Langthjem, M. A., Sugiyama, Y., 2000b, "Dynamic Stability of Columns Subjected to Follower Loads: A Survey", Journal of Sound and Vibration, 238 (5), 809-851.

Pedersen, P, Seyranian, A. P., 1983, "Sensitivity Analysis for Problems of Dynamic Stability", Internationa Journal of Solid and Structures, 19, 315-335.

Sugiyama, Y., Langthjem, M. A., Ryu, B.-J., 1999, "Letters to the Editor – Realistic Follower Forces", Journal of Sound and Vibration, 225 (4), 779-782.

Sugiyama, Y., Katayama, K. and Kiriyama, K., 2000, "Experimental Verification of Dynamic Stability of Vertical Cantilevered Columns Subjected to a Sub-Tangential Force", Journal of Sound and Vibration, 236 (2), 193-207.

Svanberg, K., 1998, "The Method of Moving Asymptotes – Modeling Aspects and Solution Schemes", Lecture notes for the DCAMM course, Advanced Topics in Structural Optimization.

Zuo, Q. H., Schreyer, H. L., 1996, "Flutter and Divergence Instability of Nonconservative Beams and Plates", Int. Journal Solid Structures, 33 (9), 1355-1367.

8. RESPONSIBILITY NOTICE

The authors are the only responsible for the printed material included in this paper.